

Influence of short-term hydrographic variations during the north-east monsoon on picophytoplankton community structure in the eastern Arabian Sea

Rajaneesh K. M., Smita Mitbavkar*, Anil A.C.

Council of Scientific and Industrial Research, National Institute of Oceanography, Dona Paula, Goa
403 004, India.

* Corresponding author: Tel.: + 91 832 2450376; Fax: + 91 832 2450615.

E-mail address: mitbavkars@nio.org (Smita Mitbavkar)

Abstract

The eastern Arabian Sea over the continental margin is a dynamic region subjected to short-term variability in hydrography as a result of various physical forcings such as coastal advection and vertical mixing. In order to assess the influence of hydrography on the picophytoplankton community, a temporal high resolution (every 3 h for nine days) study was carried out at a fixed location (15° 18' 46"N, 72° 41' 53"E) in the eastern Arabian Sea during the early north-east monsoon (November 2011). The picophytoplankton community comprised of *Synechococcus*, *Prochlorococcus*, and picoeukaryotes. Based on the temperature and salinity distribution, the study period was divided into phase I representing a stratified water column and phase II representing a vertically mixed water column. Phase I had higher picophytoplankton abundance with the initial dominance of *Prochlorococcus* which was later taken over by picoeukaryotes. Towards the end of phase I, with the initiation of vertical mixing, picoeukaryotes were the first to respond to the nutrient influx. As the vertical mixing intensified during phase II, the picophytoplankton abundance declined. Picophytoplankton carbon biomass and their contribution to total phytoplankton biomass was relatively higher during phase I with picoeukaryotes as the major contributors. These transient variations in picophytoplankton abundance highlights the importance of high frequency observations at the single cell level for better understanding the population dynamics in such environments.

Keywords: eastern Arabian Sea; picophytoplankton; community structure; hydrography; high resolution sampling; environmental factors

1. Introduction

The Arabian Sea (AS) constitutes the north-western part of the Indian Ocean and its semi-enclosed feature leads to an unusual climate, hydrography, and biogeochemical processes (Naqvi et al., 2003). As a result of the semiannual reversal of monsoon winds, seasonal variation of water column characteristics is also observed (Qasim, 1982; Banse, 1987). During the south west monsoon (SWM), coastal upwelling is a common phenomenon (Banse, 1968; Banse and McClain, 1986; Shetye et al., 1994) whereas during the north-east monsoon (NEM) convective mixing is prominent in the northern AS (Madhupratap et al., 1996) with decreasing intensity of mixing towards the southern AS (Prasanna Kumar et al., 2000). Additionally, during this period downwelling is also observed (Rao et al., 2008). Monsoonal forcing results in seasonal variations in the mixed layer depth, flux of nutrients to the upper mixed layer and thereby on pelagic food web structure and production (Madhupratap et al., 1996; Morrison et al., 1998; Prasanna Kumar et al., 2000; Wiggert et al., 2000; Shankar et al., 2005).

In the AS, phytoplankton biomass and primary productivity are high during the SWM and the NEM (Marra et al., 1998; Prasanna Kumar et al., 2000). During the NEM, interannual variations in the phytoplankton biomass and primary production are significant along the eastern (Bhattathiri et al., 1996; Sawant and Madhupratap, 1996; Parab et al., 2006; Ahmed et al., 2016) and the western AS (Campbell et al., 1998; Brown et al., 1999; Garrison et al., 2000). Only a few of the above studies have dealt with the smaller sized phytoplankton groups in the eastern AS (Roy et al., 2015; Ahmed et al., 2016).

During the last decades, the importance of picophytoplankton (PP; $< 3 \mu\text{m}$) has been demonstrated in the marine environment as major contributors to the phytoplankton biomass (Worden et al., 2004; Richardson and Jackson, 2007). PP comprises of three major groups, *Prochlorococcus* (*PRO*), *Synechococcus* (*SYN*) and picoeukaryotes (PEUK). *PRO* dominates the oligotrophic waters and is encountered down to 150 m depth (Chisholm et al., 1988; Partensky et al., 1999; Johnson et al., 2006; Fuller et al., 2006). *SYN* is abundant in mesotrophic waters with a shallower vertical distribution than that of *PRO* (Bouman et al., 2006; Zwiirglmaier et al., 2007; Flombaum et al., 2013). PEUK, along with *SYN* dominate the nutrient-rich coastal ecosystems (Blanchot et al., 2001; Jiao et al., 2005; Sharples et al., 2009). Although limited information is available on the PP community from the eastern AS, short-term variability which can impart an in-depth understanding of the PP dynamics still remains unknown.

In this study, we focused on the short-term vertical variations (every 3 h for 9 days) in the PP community structure at a fixed location over the continental slope in the eastern AS, off Goa, India. The objective of this study was to assess the influence of different hydrographic conditions such as stratification and mixing on the PP distribution pattern. We hypothesize that in the eastern AS, the PP community structure and carbon biomass varies in response to the short-term hydrographic variability resulting from coastal advection and vertical water column mixing. This study will also serve as a basis for understanding the response of phytoplankton community as a whole with chlorophyll biomass as the proxy.

2. Materials and methods

2.1. Sampling

Sampling was conducted for 9 days (D) at an interval of 3 h at one fixed location over the continental slope of the eastern AS (15° 18' 46"N, 72° 41' 53"E) (Fig. 1), onboard the ocean research vessel ORV Sindhu Sankalp (SSK-27) during the early NEM season (18-26 November 2011). Temperature, salinity and dissolved oxygen (DO) data profiles were taken from precalibrated CTD. Mixed layer (ML) depth was derived from the sigma-t criteria, as the depth at which a change from the surface sigma-t of 0.125 has occurred. Water samples for nutrients and PP analyses were collected from 7 to 10 depths in the upper 0 - 200 m water column with 12 dm³ Niskin bottles (General Oceanics, Miami, FL, USA) mounted on a CTD (Sea- Bird electronics) rosette sampler. Nutrient samples were analyzed [nitrite (NO₂⁻), nitrate (NO₃⁻), orthophosphate (PO₄³⁻), ammonium (NH₄⁺), and silicate (SiO₄⁴⁻)] with a SKALAR SAN^{plus} auto-analyzer. For analysis of PP, water samples were preserved in paraformaldehyde (final concentration 0.2%; Campbell, 2001). After 15 min dark incubation, the samples were quick-frozen in liquid nitrogen and stored at -80°C until analysis. For chlorophyll *a* analysis, water samples (~3-4 L) were filtered through GF/F filter followed by extraction of pigments in 90% acetone which were measured using High Performance Liquid Chromatography (LC 1200 series, Agilent Technologies, USA; Acharyya et al., 2012).

2.2. Flow cytometric analyses of picophytoplankton

In the laboratory, samples were thawed and analyzed through FacsVerse flow cytometer configured with 20 mW and 40 mW air-cooled lasers exciting at 488 nm (blue) and 664 nm (red), respectively. Sample acquisition was set for 10000 events. Flow rates were calibrated before analysis using the equation, $R = (W_i - W_f) / (T \times d)$ where W_i = initial weight of the sample (mg), W_f = final weight of the sample (mg), T = time (minutes), and d = density of the sample (seawater = 1.03) (Marie et al., 2005). Forward angle light scatter (FALS; proxy for cell size) and right angle light

scatter (RALS), orange (564-606 nm) and red (> 650 nm) fluorescence intensities were collected from each particle and analyzed with FACS Suite™ software. Yellow-green fluoresbrite fluorescent beads (Polysciences co., USA) of 2 μm diameter were added to the samples as an internal standard. Cell fluorescence emission and light scatter signals of each PP group were normalized to that of the beads (mean cell values/ mean bead values) to distinguish the different PP groups based on their autofluorescence properties and size. Three major groups of PP were determined (Fig. 2a-c). *SYN* was identified based on the orange fluorescence of the pigment phycoerythrin. PEUK were differentiated from *PRO* based on the relatively higher red chl *a* fluorescence and largest FALS.

2.3. Carbon biomass estimation

Phytoplankton carbon biomass was derived from chl *a* using a carbon: chl *a* ratio of 140 and 83 $\mu\text{g C} : \mu\text{g chl}^{-1}$ for the phase-I and phase-II ML depths, respectively (Shalapyonok et al., 2001). A C: chl *a* ratio of 52 was used for depths below the ML (Brown et al., 1999; Garrison et al., 2000). Carbon biomass of *SYN*, *PRO* (Garrison et al., 2000; Shalapyonok et al., 2001) and PEUK (Shalapyonok et al., 2001) were estimated using conversion factors as given in Table 1. For PEUK, the biovolume calculated from FALS was converted to carbon per cell (Shalapyonok et al., 2001).

2.4. Data analyses

The depth of euphotic zone ($Z_{1\%}$) was estimated from chl *a* concentration of surface layer using the chl centered approach (Lee et al., 2007). The percentage contribution of PP to total phytoplankton carbon biomass and individual PP group contribution to total PP carbon biomass were estimated from the phytoplankton and PP carbon values. PP carbon biomass was depth integrated by trapezoidal method and its percentage contribution to the total phytoplankton biomass was also calculated.

PERMANOVA analysis (Wood et al., 2016) was performed using PRIMER 6 software to assess the variation in the biotic (*SYN*, *PRO*, PEUK, PP carbon biomass, chl *a*, phytoplankton carbon biomass, and PP carbon contribution) and abiotic (nutrients, temperature, salinity, and DO) parameters between phase I (stratified water column) and phase II (mixed water column) samplings in the surface (0 m), ML and below ML. Path analysis was used to explain the linear relationships (R^2 = coefficient of determination) between the biological and the contextual physicochemical parameters in the ML (phase I and phase II) and below ML (50 m, 75 m and 100 m depths). It was conducted as a hierarchical multiple regression analysis and the obtained results were used to establish a path diagram (SPSS Amos). The D5 data (ML and below ML) was also treated separately in order to assess the PP response to environmental conditions during the transition phase.

3. Results

3.1. Environmental variables

Based on the ML depth, the sampling period was divided into two phases: phase I (from D1 to D5) was characterized by a shallow ML (25.58 ± 4.85 m) with high temperature ($29.39 \pm 0.2^\circ\text{C}$) and low salinity (34.34 ± 2.8) water mass, and phase II (D6 to D9) was characterized by a deep ML (51.44 ± 5.50 m) with lower temperature ($28.62 \pm 0.2^\circ\text{C}$) and higher salinity (35.15 ± 0.43) water mass (Fig. 3a, b). DO concentration ranged from 3.9 to 6.1 mg dm^{-3} in the ML (Fig. 3c). Nutrient concentrations within the ML were significantly higher during phase II. NO_3^- and PO_4^{3-} concentrations were $<1 \mu\text{M}$ within the ML during phase I whereas during phase II, it increased ($>1 \mu\text{M}$; Fig. 3d, Fig. 3f). PO_4^{3-} concentration started increasing from the end of phase I (D4-D5; Fig. 3f). NO_2^- concentration ranged from 0.02 to 0.97 μM in the water column (Fig. 3e). SiO_4^{4-} concentration in the ML ranged from 1.05 to 6.54 μM (Fig. 3g). In the ML, NH_4^+ concentration ranged from 0.01 to 5.95 μM (Fig. 3h). Nutricline deepened during the beginning of phase I and during phase II, whereas it was shallower during end of phase I (D4-D5). The depth of euphotic layer ranged between 60 and 70 m during the study period.

3.2. Picophytoplankton community structure

Variations of hydrographic conditions during the two phases were well reflected in the PP community structure and its abundance, especially in the ML. At the beginning of phase I, *SYN* abundance was higher in the upper 75 m water column, with maximum abundance at 50 m (6.4×10^4 cells cm^{-3}). Its abundance reduced during the later part of phase I (except on D4 at 25 m; 9.8×10^4 cells cm^{-3}) and phase II (Fig. 4a). At the beginning of phase I, *PRO* was the dominant PP group in the water column. *PRO* population was observed down to 200 m depth with maximum abundance in the ML and occasionally in deeper waters (100 m; Fig. 4b). By the end of phase I, PEUK was the dominant PP group, especially between 25 m and 75 m depths (Fig. 4c). On D5 and D6, dominance of PEUK extended to deeper waters (75 m). PEUK had a higher abundance at 50 m, except on D2 and D3. During phase II, the abundance of all PP groups ($PRO > PEUK > SYN$) reduced by an order of magnitude in the water column. Overall, PP abundance was higher during phase I (Fig. 4d).

Pronounced diel variation was observed in the PP community during the study period. Generally, *SYN*, *PRO*, and PEUK showed higher cell abundance during the afternoon and night (12:00 to 24:00) and the time of attaining maximum cell abundance showed variation between the two phases. In particular, during phase I (D1 to D3) the abundance of *SYN*, *PRO*, and PEUK was higher at 18:00, 15:00, and 12:00, respectively, which remained high till 24:00 (Fig. 4a-c). At the end of phase I,

PEUK cell abundance was higher at 9:00 but *SYN* and *PRO* did not show any change in the pattern. During phase II, in the ML, higher abundance of *SYN* and *PRO* was observed at 12:00 and PEUK at 15:00 (Fig. 4a-c). In both phases, higher abundance of *SYN* and PEUK was only observed in the upper 50 m (Fig. 4a, Fig. 4c). *PRO* abundance was higher in the shallower depths (upper 50 m) from evening to night (after 15:00) and below 50 m depth before 15:00 during phase I, whereas, during phase II, higher cell abundance was observed only in the upper 50 m (Fig. 4b).

3.3. Contribution of picophytoplankton to the total phytoplankton carbon biomass

Chl *a* concentration ranged from 0.07 to 1.09 $\mu\text{g dm}^{-3}$ with peak values just below the ML (50 m; Fig. 5a). Chl *a* concentrations were high during afternoon and night followed by lower values in the early morning. Phytoplankton carbon biomass varied from 2.5 to 203.1 $\mu\text{g dm}^{-3}$ in the water column with higher concentrations below the ML. Phytoplankton carbon biomass concentration was significantly ($P < 0.05$) higher during phase I than phase II in the ML and also below ML. PP carbon biomass varied from 0.1 to 98.32 $\mu\text{g dm}^{-3}$ in the water column during the entire study period (Fig. 5b). PP contribution to the total phytoplankton carbon in the entire water column ranged from 13 to 70% during phase I and 15 to 47% during phase II. Higher PP carbon contribution was observed during phase I, especially on D5 (26 - 70%, entire water column, Fig. 5c). Depth-integrated PP carbon biomass concentration was significantly ($P < 0.05$) higher during phase I than phase II in surface, ML and below ML. Depth-integrated PP carbon biomass contribution to the total phytoplankton carbon ranged from 9 to 58% in the ML during the entire study period. However, there was not much difference in their contribution to total phytoplankton carbon biomass in surface and ML; whereas below ML, PP carbon contribution to total carbon biomass was higher during phase I than phase II.

At the end of phase I, the PP carbon biomass was higher especially at 25 m and 50 m depth with a major contribution by PEUK (Fig. 6c). The major contributor to PP carbon biomass was PEUK (35 - 90%) followed by *SYN* (4 - 44%) and *PRO* (1-39%) in the upper 50 m during both phases (Fig. 6a-c). In the deeper waters, *PRO* carbon biomass was dominant except at the end of phase I, where PEUK was dominant down to 100 m depth. However, on some occasions, *PRO* dominated the PP carbon biomass in the ML. There was no consistent diel pattern of PP carbon biomass and its contribution to the total phytoplankton carbon biomass. Generally, PP contribution was higher in the upper 50 m depth but at the end of phase I, higher PP carbon contribution was observed down to 100 m, and extended down to 150 m in the early phase II.

3.4. Relationship between picophytoplankton and environmental variables

PERMANOVA analysis revealed significant variations ($P < 0.01$) in temperature, DO, PO_4^{3-} , SiO_4^{4-} , chl *a* concentration, PEUK abundance, *PRO* abundance, phytoplankton carbon biomass, and PP carbon biomass between phase I and phase II samplings in the surface waters (0 m) whereas salinity, NH_4^+ , NO_2^- , NO_3^- and PP contributions showed insignificant variations (Table 2). In ML, significant variations ($P < 0.01$) were observed in temperature, nutrient concentrations, chl *a* concentration, PP group cell abundances, phytoplankton carbon biomass, and PP carbon biomass between phase I and phase II samplings whereas salinity, DO and PP contributions showed insignificant variations (Table 2). Below ML, DO, nutrients (except SiO_4^{4-}), chl *a* concentration, *SYN*, PEUK, phytoplankton carbon biomass, PP carbon biomass and its contribution to total phytoplankton carbon biomass showed significant variation ($P < 0.01$) between phase I and phase II samplings, whereas temperature, salinity, *PRO* abundance and SiO_4^{4-} showed insignificant variations (Table 2).

In the ML, variability of *SYN* abundance was partially explained by the positive correlation with temperature and NO_3^- during phase I ($R^2 = 0.17$, $P < 0.05$) and PO_4^{3-} during phase II ($R^2 = 0.12$, $P < 0.05$) (Fig. 7a, b). The variation of PEUK abundance was partially explained by negative correlation with temperature, and positive correlation with PO_4^{3-} and NO_3^- during phase I ($R^2 = 0.33$, $P < 0.05$) and positive correlation with NH_4^+ , salinity, and temperature during phase II ($R^2 = 0.28$, $P < 0.05$). *PRO* abundance variation was partially explained by the positive correlation with temperature and NO_2^- during phase I ($R^2 = 0.23$, $P < 0.05$) and negative correlation with NH_4^+ and positive correlation with PO_4^{3-} during phase II ($R^2 = 0.12$, $P < 0.05$). The variability of PP carbon biomass was largely explained by positive correlation with *SYN*, PEUK, temperature and nutrient concentrations (NH_4^+ , PO_4^{3-} , NO_2^- and NO_3^-) during phase I ($R^2 = 0.93$, $P < 0.05$) and positive correlation with PEUK, *PRO*, PO_4^{3-} , and NO_3^- ; and negative correlation with NH_4^+ and temperature during phase II ($R^2 = 0.83$, $P < 0.05$). The variation in phytoplankton carbon biomass was largely explained by positive correlation with PP carbon biomass and PO_4^{3-} and negative correlation with salinity, SiO_4^{4-} and NO_2^- during phase I ($R^2 = 0.67$, $P < 0.05$) and positive correlation with PP carbon biomass and salinity during phase II ($R^2 = 0.73$, $P < 0.05$) (Fig. 7a, b).

At 50 m depth, variation in *SYN* abundance was largely explained by the positive correlation with temperature ($R^2 = 0.32$, $P < 0.05$), at 75 m, partially explained by the negative correlation with NH_4^+ ($R^2 = 0.16$, $P < 0.05$) and at 100 m depth, largely explained by the positive correlation with salinity, NO_2^- and NO_3^- and negative correlation with temperature and PO_4^{3-} , ($R^2 = 0.47$, $P < 0.05$; Fig. 7c-e). The variation in PEUK abundance at 50 m depth was largely explained by the positive correlation with NH_4^+ , SiO_4^{4-} , and PO_4^{3-} , and negative correlation with NO_3^- ($R^2 = 0.51$, $P < 0.05$), at 75 m by

the positive correlation with salinity and negative correlation with temperature and PO_4^{3-} ($R^2 = 0.33$, $P < 0.05$) and 100 m depth, partially by the positive correlation with NO_3^- ($R^2 = 0.14$, $P < 0.05$). The variation in *PRO* abundance was largely explained by the positive correlation with temperature and NH_4^+ at 50 m depth ($R^2 = 0.53$, $P < 0.05$), whereas at 75 m by the positive correlation with temperature ($R^2 = 0.13$, $P < 0.05$). At 50 m, variation in PP carbon biomass was largely explained by the positive correlation with PEUK, NO_3^- and NH_4^+ and negative correlation with SiO_4^{4-} ($R^2 = 0.73$, $P < 0.05$), at 75 m, largely explained by the negative correlation with salinity and positive correlation with PEUK abundance and temperature ($R^2 = 0.65$, $P < 0.05$) and at 100 m, largely explained by the positive correlation with PEUK abundance ($R^2 = 0.41$, $P < 0.05$). At 50 m, the positive correlation with PP carbon biomass largely explained the variation in phytoplankton carbon biomass ($R^2 = 0.42$, $P < 0.05$), at 75 m, largely explained by the positive correlation with PP carbon biomass and negative correlation with NO_3^- ($R^2 = 0.43$, $P < 0.05$) and at 100 m depth, largely explained by the positive correlation with salinity and PP carbon biomass ($R^2 = 0.40$, $P < 0.001$).

On D5, variability of *SYN* abundance was largely explained by the positive correlation with temperature, PO_4^{3-} and NO_3^- in ML ($R^2 = 0.82$, $P < 0.05$; Fig. 7f), whereas below ML by the positive influence of salinity, temperature and NO_3^- and negative correlation with PO_4^{3-} ($R^2 = 0.96$, $P < 0.05$; Fig. 7g). The variation in PEUK abundance was largely explained by the positive correlation with temperature, NH_4^+ , PO_4^{3-} , and NO_3^- and negative correlation with NO_2^- in ML ($R^2 = 0.88$, $P < 0.05$); whereas below ML by the positive correlation with temperature, NH_4^+ , SiO_4^{4-} , and PO_4^{3-} and negative correlation with salinity, NO_2^- , and NO_3^- ($R^2 = 1.00$, $P < 0.05$). The variation in *PRO* abundance in the ML was largely explained by the positive correlation with PO_4^{3-} and temperature ($R^2 = 0.67$, $P < 0.05$) whereas below ML, by the positive correlation with PO_4^{3-} , and negative correlation with NO_3^- and NH_4^+ ($R^2 = 0.77$, $P < 0.05$). The variability of PP carbon biomass was largely explained by the positive correlation with salinity, temperature, PO_4^{3-} , NO_2^- , NO_3^- , PEUK and *PRO* and negative correlation with *SYN* and SiO_4^{4-} in the ML ($R^2 = 1.00$, $P < 0.05$) whereas below ML by a positive correlation with NO_2^- , NO_3^- , and PEUK and negative correlation with NH_4^+ , SiO_4^{4-} , PO_4^{3-} and *PRO* ($R^2 = 1.00$, $P < 0.05$). The variation in phytoplankton carbon biomass ($R^2 = 0.92$, $P < 0.05$) was largely explained by the positive correlation with PP carbon biomass and negative correlation with salinity, PO_4^{3-} and NH_4^+ in the ML, whereas below ML, by the positive correlation with PP carbon biomass, temperature and NO_3^- and negative correlation with salinity, SiO_4^{4-} and PO_4^{3-} ($R^2 = 1.00$, $P < 0.05$).

4. Discussion

4.1. Variations in picophytoplankton community structure

There is a scarcity of information on the short-term variability in PP (Jacquet et al., 2002), especially in the AS where monsoonal winds influence the hydrography. Hence a high resolution study at a fixed station over the continental slope of the eastern AS was carried out to better understand the impact of short-term variability in hydrography and environmental conditions on the PP community dynamics. During this study, the dynamic hydrography was well reflected in the PP community structure. The ML depth evolved from shallow (phase I) to deep (phase II). The relatively lower salinity (34) surface waters during phase I could be attributed to the advection of low saline coastal waters (Shankar et al. 2005). The resultant oligotrophic conditions during phase I favored *PRO* and *SYN* growth within the mixed layer (Anderson et al., 2008; Dongen-Vogels et al., 2012), with *PRO* as the dominant group. In the north western AS and Alboran Sea, *SYN* and PEUK dominated the mesotrophic conditions whereas oligotrophic conditions were dominated by *PRO* (Campbell et al., 1998; Jacquet et al., 2002). Generally, in surface waters, *PRO* cells are better adapted to high temperature, low nutrient and stratified water column (Campbell et al., 1998; Liu et al., 1998; Zubkov et al., 1998; Agawin et al., 2000; Jiao et al., 2005). This is also supported by path analysis where *PRO* positively correlated with temperature but showed an insignificant relation with NO_3^- and PO_4^{3-} within the mixed layer. The degree of mixing in euphotic layer of the water column was also associated with differences in temperature of around 30°C in the mixed layer compared with 25°C at 50-75 m. Hence, the temperature of each layer could have influenced the *PRO* populations in the euphotic layer. Below the mixed layer, the positive correlation of *PRO* with the prevailing temperature at 50 m and 75 m suggests the influence of this parameter on its vertical distribution. Different ecotypes of *PRO* such as high light (HL) and low light (LL) adapted have been reported in the oceanic waters (Partensky et al., 1993; Moore and Chisholm, 1999). Depending on their ability to adapt to different light optima for growth, HL ecotype dominates in the surface waters and LL ecotype in the deeper waters (Partensky et al., 1999). Similar observations have been reported from the NEAS (Roy and Anil, 2015). As the euphotic depth in the present study area ranged between 60 and 70 m, vertical distribution of light could have played an important role in the distribution of HL and LL adapted *PRO* strains.

SYN, the next abundant group during phase I, which correlated positively with the prevailing temperature within the mixed layer (30°C) and at 50 m (25°C) suggests a temperature maxima regulating its vertical distribution in the water column. In the deeper waters (75-100 m), its minimal abundance in spite of the high nutrient concentrations could be due to lowered growth rates. Since *SYN* is a mesotrophic form, its vertically decreasing trend shows that temperature and irradiance effect overrides the nutrient needs to optimize growth (Mouriño-Carballido et al., 2016). Another

loss factor resulting in its lower abundance could be the high grazing pressure exerted by the small heterotrophic nanoflagellates (Reckermann and Veldhuis, 1997). The vertical distribution of the least abundant group, PEUK, were generally controlled by the nutrients as seen from the positive correlation. PEUK are the main carbon source for the microzooplankton (Reckermann and Veldhuis, 1997). However, the role of grazers as the controller of PEUK in the open oceans is unclear (Hirose et al., 2008). PEUK mortality losses (50-100%) due to viral lysis was also reported with rates ranging from 0.1 to 0.8 d⁻¹ (Baudoux et al., 2007).

With the initiation of vertical mixing during the transition phase (D5) at the end of phase I, increased abundance of the PP groups within the mixed layer, with *SYN* dominating the community, suggests a positive influence of increased nutrient concentrations. This was supported by the positive correlation with the prevailing temperature, NO₃⁻ and PO₄³⁻. Below the ML, the highest PEUK abundance at the subsurface chl *a* maxima where *SYN* and *PRO* exhibited relatively lower numbers, coincided with increased nutrient concentrations. This was supported by the positive correlation of PEUK with nutrients (SiO₄⁴⁻, PO₄³⁻, and NH₄⁺). During this period, PEUK cell abundance peaked earlier than that of *PRO* and *SYN*, implying cell division, which could be mainly driven by variations in nutrient concentrations. This also suggests that during pulses of nutrient inputs, PEUK are the fastest to respond amongst the PP groups, followed by *PRO*. Amongst the larger phytoplankton, diatoms respond to pulsed nutrient inputs (Ornolfsdottir et al., 2004). Some diatom species such as *Chaetoceros thronsdensei* which attain a minimum size of 1.5 µm have also been observed in the PP community (Vaulot et al., 2008). Not et al. (2008) also reported the presence of picoplanktonic diatom in Indian ocean. *Minutocellus* species, strains RCC703 which belongs to Bacillariophyceae was isolated from Indian ocean (Giovagnetti et al., 2012). However, till date there is no published data suggesting that pico-diatoms are an important fraction of the picophytoplankton in the present study area. The positive correlation of PEUK with SiO₄⁴⁻ implies representation by some smaller diatoms that are quick in responding to nutrient pulses due to their greater capacity for assimilation of nutrients at high concentrations (Agawin et al., 2000; Jiao et al., 2005; Paulsen et al., 2015). The present study area was located above the continental slope, and usually, at the continental shelf break and slope, formation of internal tides and nonlinear waves (Smith and Sandstrom, 1988; Shenoi and Antony, 1991; Shankar et al., 2005), cause churning of water column (Wolanski and Pickard, 1983; Kurapov et al., 2010) that results in nutrient influx from the sediment to the upper water column yielding high productivity (Sharples et al., 2001). In the shelf edge of north east Atlantic Ocean complete dominance of PEUK was observed due to the supply of NO₃⁻ from bottom waters, whereas *SYN* and *PRO* were dominant in the NO₃⁻ depleted continental shelf region (Sharples et al., 2009).

Dongen-Vogels et al. (2011) observed that the mixing process decreases the light irradiance and increases the nutrient input which led to a proliferation of eukaryotes and decline of prokaryotes. The PEUK abundance was the highest recorded for the entire study period and also coincided with the higher chl *a* biomass below the ML. Their contribution to the total phytoplankton biomass (26 - 70%) implies that PEUK were the major contributors. Sharples et al. (2009) reported a higher rate of primary production in the shelf edge, which can support higher trophic levels including fishes, thereby serving as a potential fishery zone. The short life span of PEUK abundance peak could be attributed to the grazing by heterotrophic nanoflagellates whose growth response is as quick as the PP (Eccleston-Parry and Leadbeater, 1994; Landry et al., 1998) leading to a succession of the phytoplankton community by diatoms. The high resolution vertical sampling strategy allowed us to capture such refined transient observations *in situ* which are essential for further understanding of the microbial loop functioning in such dynamic ecosystems.

The vertical mixing of water column during phase II caused deepening of the mixed layer leading to a uniform distribution of PP within the ML, with significantly lower PP abundance and biomass compared to phase I. On the other hand, phytoplankton biomass did not vary much during this period. This suggests that during vertical mixing, increased nutrient concentration favored larger phytoplankton. However, the prevalence of lower numbers of PP for a longer period of time (4 days) suggests lowered growth rates due to certain unfavorable environmental perturbation due to deepening of ML. In addition to the physical factors, the observed diel patterns in *SYN*, *PRO* and PEUK abundance could be attributed to biological factors such as cell division, cell death and loss factors such as grazing, viral infection and parasitism (Crompton and Wetzel, 1982; Banse, 1994; Vaulot and Marie, 1999; Behrenfeld, 2010). The biological processes are in turn driven by nutrient or irradiance availability. The dephased abundance peaks for the three PP groups during the day time could be attributed to the cell division and the decreasing cell abundance during the night to higher grazing pressure (Reckermann and Veldhuis, 1997; Partensky et al., 1999; Gauns et al., 2005). As the cells divide their reduced size makes them more vulnerable to predation (Tsai et al., 2005).

4.2. Picophytoplankton carbon biomass

The appropriate selection of the C:Chl *a* ratios and carbon cell conversion factors for PP from that reported in literature is a challenging task as they are known to vary with growth conditions (Booth et al., 1993; Buck et al., 1996; Taylor et al., 1997). As such, the values determined in the open ocean are more realistic than in cultures. Taking into consideration the contrasting conditions under which the sampling was conducted, the closest match was found in Garrison et al. (2000) and Shalapyonok et al. (2001). This study was carried out in the AS during NEM wherein carbon cell⁻¹ for both *PRO*

and *SYN* varied significantly between cells from within and below ML, which was in the range observed in our study (< 50 m). For the C:Chl *a* ratios in ML, we used the upper (for phase I) and lower (for phase II) limits of the average value (112 ± 29 ; Shalapyonok et al., 2001). For below ML, we used a factor (52) suggested by Brown et al. (1999) and Garrison et al. (2000) for the AS when the ML was > 50 m. The relative contribution of the PP carbon to total phytoplankton carbon biomass (up to 70%) obtained by this approach was consistent with the previous studies carried out in the AS during NEM (Shalapyonok et al., 2001). Using lower factors led to over estimation of the carbon values. Thus, these biomass assessments can be considered reliable and useful for further PP studies in these waters.

The PP carbon biomass contribution to total carbon biomass increases in these waters when stratified conditions prevail. On the other hand, the vertical mixing and the associated deepening of the surface layer lead to a decrease of PP carbon biomass indicating that increasing mixed layer depth is less supportive for PP growth (Lindell and Post, 1995). This tendency suggests that mixing of the water column contributes to the maintenance of large cells such as diatoms in the water column, since diatoms are otherwise subjected to high sinking losses, as observed earlier in the AS (Campbell et al., 1998). These variations were driven by the gradual increase in nutrient concentration due to vertical mixing, from phase I to II as was evident from the positive correlation of chl *a* and phytoplankton carbon biomass with nutrients. Higher abundance of *SYN* and PEUK coincided with the maximum chl *a* peak signifying that the total phytoplankton biomass was largely contributed by PP. This is also evident from a significant positive relation between total phytoplankton carbon biomass and PP carbon biomass. The major component of PP carbon biomass was PEUK (35 - 90%) even though their abundance was low. This is mainly due to their larger size compared to *PRO* and *SYN* (Buitenhuis et al., 2012). Through this study it is evident that transient bursts in PP abundance can be captured *via* high resolution sampling which can be missed during the spatial observations depending on the sampling time. The short duration of these abundance peaks suggest incorporation of this biomass into higher trophic levels. Future high resolution studies at different regions in the continental margin encompassing the other components of the food web will help in validating and better elucidating the PP responses under varying environmental conditions.

Acknowledgements

The authors would like to thank the Director of Council of Scientific and Industrial Research (CSIR)-National Institute of Oceanography for his support. The authors wish to acknowledge Mr. Sundar D., chief scientist of the SSK-27 cruise and Mr. Michael G.S., for providing CTD data. We thank Dr. V.V.S.S. Sarma for providing chlorophyll *a* (HPLC derived) data. We thank Dr. Shankar

D. for the support and encouragement. We thank Mr. S. Subha Anand for providing nutrient data and our project team members for their help and suggestions during sampling. We would also like to thank the officers and crew of the SSK-27 cruise for onboard help. We thank the anonymous reviewers for their valuable comments. Rajaneesh K.M. acknowledges CSIR for the award of Senior Research Fellowship. This work was funded by the project Ocean Finder (PSC 0105). This is NIO contribution (no.----).

References

- Acharyya, T., Sarma, V. V. S. S., Sridevi, B., Venkataramana, V., Bharathi, M. D., Naidu, S.A., Kumar, B. S. K., Prasad, V. R., Bandyopadhyay, D., Reddy, N. P. C., Kumar, M.D., 2012. Reduced river discharge intensifies phytoplankton bloom in Godavari estuary, India. *Mar. Chem.*, 132: 15-22
- Agawin, N. S., Duarte, C. M., Agusti, S., 2000. Nutrient and temperature control of the contribution of picoplankton to phytoplankton biomass and production. *Limnol. Oceanogr.*, 45: 591-600
- Ahmed, A., Kurian, S., Gauns, M., Chndrasekhararao, A. V., Mulla, A., Naik, B., Naik, H., Naqvi, S.W., 2016. Spatial variability in phytoplankton community structure along the eastern Arabian Sea during the onset of south-west monsoon. *Cont. Shelf Res.*, 119: 30-39
- Anderson, C. R., Siegel, D. A., Brzezinski, M. A., Guillocheau, N., 2008. Controls on temporal patterns in phytoplankton community structure in the Santa Barbara Channel, California. *J. Geophys. Res.*, 113: 1-16
- Banse, K., 1968. Hydrography of the Arabian Sea shelf of India and Pakistan and effects on demersal fishes. *Deep Sea Res.*, 15: 45-79
- Banse, K., McClain, C., 1986. Winter blooms of phytoplankton in the Arabian Sea as observed by the Coastal Zone Color Scanner. *Mar. Ecol. Prog. Ser.*, 34: 201-211
- Banse, K., 1987. Seasonality of phytoplankton chlorophyll in the central and northern Arabian Sea. *Deep Sea Res. Pt A.*, 34: 713-723
- Banse, K., 1994. Grazing and zooplankton production as key controls of phytoplankton production in the open ocean. *Oceanography*, 7: 13-20
- Baudoux, A. C., Veldhuis, M. J., Witte, H. J., Brussaard, C. P., 2007. Viruses as mortality agents of picophytoplankton in the deep chlorophyll maximum layer during IRONAGES III. *Limnol. Oceanogr.*, 52: 2519-2529
- Behrenfeld, M. J., 2010. Abandoning Sverdrup's critical depth hypothesis on phytoplankton blooms. *Ecology*, 91: 977-989
- Bhattachiri, P., Pant, A., Sawant, S., Gauns, M., Matondkar, S. G. P., Mahanraju, R., 1996. Phytoplankton production and chlorophyll distribution in the eastern and central Arabian Sea in 1994-1995. *Curr. Sci.*, 71: 857-862

- Blanchot, J., André, J.-M., Navarette, C., Neveux, J., Radenac, M. H., 2001. Picophytoplankton in the equatorial Pacific: vertical distributions in the warm pool and in the high nutrient low chlorophyll conditions. *Deep Sea Res. I*, 48: 297-314
- Booth, B. C., Lewin, J., Postel, J. R., 1993. Temporal variation in the structure of autotrophic and heterotrophic communities in the subarctic Pacific. *Prog. Oceanogr.*, 32: 57-99
- Bouman, H. A., Ulloa, O., Scanlan, D. J., Zwirgmaier, K., Li, W. K., Platt, T., Lutz, V., 2006. Oceanographic basis of the global surface distribution of *Prochlorococcus* ecotypes. *Science*, 312: 918-921
- Brown, S. L., Landry, M. R., Barber, R. T., Campbell, L., Garrison, D. L., Gowing, M. M., 1999. Picophytoplankton dynamics and production in the Arabian Sea during the 1995 Southwest Monsoon. *Deep Sea Res. II*, 46: 1745-1768
- Buck, K. R., Chavez, F. P., Campbell, L., 1996. Basin-wide distributions of living carbon components and the inverted trophic pyramid of the central gyre of the North Atlantic Ocean, summer 1993. *Aquat. Microb. Ecol.*, 10: 283-298
- Buitenhuis, E. T., Li, W. K., Vaultot, D., Lomas, M. W., Landry, M. R., Partensky, F., Karl, D. M., Ulloa, O., Campbell, L., Jacquet, S., Lantoiné, F., Chavez, F., Macias, D., Gosselin, M., McManus, G. B., 2012. Picophytoplankton biomass distribution in the global ocean. *Earth Sys. Sci. Data*, 4: 37-46
- Campbell, L., Landry, M., Constantinou, J., Nolla, H. A., Brown, S. L., Liu, H., Caron, D. A., 1998. Response of microbial community structure to environmental forcing in the Arabian Sea. *Deep Sea Res. II*, 45: 2301-2325
- Campbell, L., 2001. Flow cytometric analysis of autotrophic picoplankton. *Methods in microbiology*, 30: 317-343
- Chisholm, S. W., Olson, R. J., Zettler, E. R., Goericke, R., Waterbury, J. B., Welschmeyer, N. A., 1988. A novel free-living prochlorophyte abundant in the oceanic euphotic zone. *Nature*, 334: 340-343
- Crumpton, W. G., Wetzel, R. G., 1982. Effects of differential growth and mortality in the seasonal succession of phytoplankton populations in Lawrence Lake, Michigan. *Ecology*, 63: 1729-1739
- Dongen-Vogels, V., Seymour, J. R., Middleton, J. F., Mitchell, J. G., Seuront, L., 2011. Influence of local physical events on picophytoplankton spatial and temporal dynamics in South Australian continental shelf waters. *J. Plankton Res.*, 20: 1-16
- Dongen-Vogels, V., Seymour, J. R., Middleton, J. F., Mitchell, J. G., Seuront, L., 2012. Shifts in picophytoplankton community structure influenced by changing upwelling conditions. *Estuar. Coast. Shelf Sci.*, 109: 81-90
- Eccleston-Parry, J. D., Leadbeater, B. S., 1994. A comparison of the growth kinetics of six marine heterotrophic nanoflagellates fed with one bacterial species. *Mar. Ecol. Prog. Ser.*, 105: 167-177
- Flombaum, P., Gallegos, J. L., Gordillo, R. A., Rincón, J., Zabala, L. L., Jiao, N., Karl, D. M., Li, W. K., Lomas, M. W., Veneziano, D., Vera, C. S., 2013. Present and future global distributions of the

marine Cyanobacteria *Prochlorococcus* and *Synechococcus*. *Proceed National Acad Sci*, 110: 9824-9829

- Fuller, N. J., Tarran, G. A., Yallop, M., Orcutt, K. M., Scanlan, D. J., 2006. Molecular analysis of picocyanobacterial community structure along an Arabian Sea transect reveals distinct spatial separation of lineages. *Limnol. Oceanogr.*, 51: 2515-2526
- Garrison, D. L., Gowing, M. M., Hughes, M. P., Campbell, L., Caron, D. A., Dennett, M. R., Shalapyonok, A., Olson, R. J., Landry, M. R., Brown, S. L., Liu, H. B., 2000. Microbial food web structure in the Arabian Sea: a US JGOFS study. *Deep Sea Res. II*, 47: 1387-1422
- Gauns, M., Madhupratap, M., Ramaiah, N., Jyothibabu, R., Fernandes, V., Paul, J. T., Kumar, S. P., 2005. Comparative accounts of biological productivity characteristics and estimates of carbon fluxes in the Arabian Sea and the Bay of Bengal. *Deep Sea Res. II*, 52: 2003-2017
- Giovagnetti, V., Cataldo, M. L., Conversano, F., Brunet, C., 2012. Growth and photophysiological responses of two picoplanktonic *Minutocellus* species, strains RCC967 and RCC703 (Bacillariophyceae). *Eur. J. Phycol.*, 47: 408-420
- Hirose, M., Katano, T., Nakano, S. I., 2008. Growth and grazing mortality rates of *Prochlorococcus*, *Synechococcus* and eukaryotic picophytoplankton in a bay of the Uwa Sea, Japan. *J. Plankton Res.*, 30: 241-250
- Jacquet, S., Prieur, L., Avois-Jacquet, C., Lennon, J. F., Vaultot, D., 2002. Short-timescale variability of picophytoplankton abundance and cellular parameters in surface waters of the Alboran Sea (western Mediterranean). *J. Plankton Res.*, 24: 635-651
- Jiao, N., Yang, Y., Hong, N., Ma, Y., Harada, S., Koshikawa, H., Watanabe, M., 2005. Dynamics of autotrophic picoplankton and heterotrophic bacteria in the East China Sea. *Cont. Shelf Res.*, 25: 1265-1279
- Johnson, Z. I., Zinser, E. R., Coe, A., McNulty, N. P., Woodward, E. M. S., Chisholm, S. W., 2006. Niche partitioning among *Prochlorococcus* ecotypes along ocean-scale environmental gradients. *Science*, 311: 1737-1740
- Kurapov, A., Allen, J., Egbert, G., 2010. Combined effects of wind-driven upwelling and internal tide on the continental shelf. *J. Phys. Oceanogr.*, 40: 737-756
- Landry, M. R., Brown, S. L., Campbell, L., Constantinou, J., Liu, H. 1998. Spatial patterns in phytoplankton growth and microzooplankton grazing in the Arabian Sea during monsoon forcing. *Deep Sea Res. II*, 45: 2353-2368
- Lee, Z., Weidemann, A., Kindle, J., Arnone, R., Carder, K. L., Davis, C., 2007. Euphotic zone depth: Its derivation and implication to ocean-color remote sensing. *J. Geophysic. Res., Oceans*, 112: 1-11
- Lindell, D., Post, A. F., 1995. Ultraphytoplankton succession is triggered by deep winter mixing in the Gulf of Aqaba (Eilat), Red Sea. *Limnol. Oceanogr.*, 40: 1130-1141
- Liu, H., Campbell, L., Landry, M., Nolla, H. A., Brown, S. L., Constantinou, J., 1998. *Prochlorococcus* and *Synechococcus* growth rates and contributions to production in the Arabian Sea during the 1995 Southwest and Northeast Monsoons. *Deep Sea Res. II*, 45: 2327-2352

- Madhupratap, M., Kumar, S. P., Bhattathiri, P., Kumar, D. M., Raghukumar, S., Nair, K. K. C., Ramaiah, N., 1996. Mechanism of the biological response to winter cooling in the northeastern Arabian Sea. *Nature*, 384: 549-552
- Marie, D., Simon, N., Vaultot, D., 2005. Phytoplankton cell counting by flow cytometry. *Algal Cultur. Techniq.*, 1: 253-267
- Marra, J., Dickey, T., Ho, C., Kinkade, C. S., Sigurdson, D. E., Weller, R. A., Barber, R. T., 1998. Variability in primary production as observed from moored sensors in the central Arabian Sea in 1995. *Deep Sea Res. II*, 45: 2253-2267
- Moore, L. R., Chisholm, S. W., 1999. Photophysiology of the marine cyanobacterium *Prochlorococcus*: Ecotypic differences among cultured isolates. *Limnol. Oceanogr.*, 44: 628-638
- Morrison, J. M., Codispoti, L., Gaurin, S., Jones, B., Manghnani, V., Zheng, Z., 1998. Seasonal variation of hydrographic and nutrient fields during the US JGOFS Arabian Sea Process Study. *Deep Sea Res. II*, 45: 2053-2101
- Mouriño-Carballido, B., Hojas, E., Cermeño, P., Chouciño, P., Fernández-Castro, B., Latasa, M., Marañón, E., Morán, X. A., Vidal, M., 2016. Nutrient supply controls picoplankton community structure during three contrasting seasons in the northwestern Mediterranean Sea. *Mar. Ecol. Prog. Ser.*, 543: 1-19
- Naqvi, S., Naik, H., Narvekar, P., 2003. The Arabian Sea. in: *Biogeochemistry of Marine Systems*, edited by: Black, K. and Shimmield, G., Blackwell, Oxford, 156-206
- Not, F., Latasa, M., Scharek, R., Viprey, M., Karleskind, P., Balagué, V., Ontoria-Oviedo, I., Cumino, A., Goetze, E., Vaultot, D., Massana, R., 2008. Protistan assemblages across the Indian Ocean, with a specific emphasis on the picoeukaryotes. *Deep Sea Res. Pt A*, 55: 1456-1473
- Ornoldsdottir, E. B., Lumsden, S. E., Pinckney, J. L., 2004. Phytoplankton community growth-rate response to nutrient pulses in a shallow turbid estuary, Galveston Bay, Texas. *J. Plankton Res.*, 26: 325-339
- Parab, S. G., Matondkar, S. P., Gomes, H. D. R., Goes, J. I., 2006. Monsoon driven changes in phytoplankton populations in the eastern Arabian Sea as revealed by microscopy and HPLC pigment analysis. *Cont. Shelf Res.*, 26: 2538-2558
- Partensky, F., Hoepffner, N., Li, W. K., Ulloa, O., Vaultot, D., 1993. Photoacclimation of *Prochlorococcus* sp. (Prochlorophyta) strains isolated from the North Atlantic and the Mediterranean Sea. *Plant Physiol.*, 101: 285-296
- Partensky, F., Hess, W., Vaultot, D., 1999. *Prochlorococcus*, a marine photosynthetic prokaryote of global significance. *Microbiol. Mol. Biol. Rev.*, 63: 106-127
- Paulsen, M. L., Riisgaard, K., Frede, T., St John, M., Nielsen, T. G., 2015. Winter-spring transition in the subarctic Atlantic: microbial response to deep mixing and pre-bloom production. *Aquat. Microb. Ecol.*, 76: 49-69
- Prasanna Kumar, S., Madhupratap, M., Dileep Kumar, M., Gauns, M., Muraleedharan, P. M., Sarma, V. V. S. S., De Souza, S. N., 2000. Physical control of primary productivity on a seasonal scale in central and eastern Arabian Sea. *J. Earth. Syst. Sci.*, 109: 433-441

- Qasim, S., 1982. Oceanography of the northern Arabian Sea. *Deep Sea Res.*, 29: 1041-1068
- Rao, A. D., Joshi, M., Ravichandran, M., 2008. Oceanic upwelling and downwelling processes in waters off the west coast of India. *Ocean Dynam.*, 58: 213-226
- Reckermann, M., Veldhuis, M. J., 1997. Trophic interactions between picophytoplankton and micro- and nanozooplankton in the western Arabian Sea during the NE monsoon 1993. *Aquat. Microb. Ecol.*, 12: 263-273
- Richardson, T. L., Jackson, G. A., 2007. Small phytoplankton and carbon export from the surface ocean. *Science*, 315: 838-840
- Roy, R., Chitari, R., Kulkarni, V., Krishna, M. S., Sarma, V. V. S. S., Anil, A. C., 2015. CHEMTAX-derived phytoplankton community structure associated with temperature fronts in the northeastern Arabian Sea. *J. Mar. Sys.*, 144: 81-91
- Roy, R., Anil, A. C., 2015. Complex interplay of physical forcing and *Prochlorococcus* population in ocean. *Prog. Oceanogr.*, 137: 250-260
- Sawant, S., Madhupratap, M., 1996. Seasonality and composition of phytoplankton in the Arabian Sea. *Curr. Sci.*, 71: 869-873
- Shalapyonok, A., Olson, R. J., Shalapyonok, L. S., 2001. Arabian Sea phyto-plankton during southwest and northeast monsoons 1995: Composition, size structure and biomass from individual cell properties measured by flow cytometry, *Deep Sea Res.*, II, 48: 1231-1261
- Shankar, D., Shenoi, S., Nayak, R., Vinayachandran, P. N., Nampoothiri, G., Almeida, A. M., Michael, G. S., Ramesh Kumar, M. R., D. Sundar, Sreejith, O. P., 2005. Hydrography of the eastern Arabian Sea during summer monsoon 2002. *J. Earth. Syst. Sci.*, 114: 459-474
- Sharples, J., Moore, C. M., Abraham, E. R., 2001. Internal tide dissipation, mixing, and vertical nitrate flux at the shelf edge of NE New Zealand. *J. Geophys. Res.*, 106: 14069–14081
- Sharples, J., Moore, C. M., Hickman, A. E., Holligan, P. M., Tweddle, J. F., Palmer, M. R., Simpson, J. H., 2009. Internal tidal mixing as a control on continental margin ecosystems. *Geophys. Res. Lett.*, 36: 1-5
- Shenoi, S. C., Antony M. K., 1991. Current measurements over the western continental shelf of India. *Cont. Shelf Res.*, 11: 81-93
- Shetye, S., Gouveia, A. , Shenoi, S., 1994. Circulation and water masses of the Arabian Sea. *Proceed. Indian Academ. Sci. Earth Planet. Sci.*, 103: 107-123
- Smith, P. C., Sandstrom, H., 1988. Physical processes at the shelf edge in the Northwest Atlantic. *J. Northwest Atlantic Fish. Sci.*, 8: 5-13
- Taylor, A. H., Geider, R. J., Gilbert, F. J., 1997. Seasonal and latitudinal dependencies of phytoplankton carbon-to-chlorophyll *a* ratios: results of a modelling study. *Mar. Ecol. Prog. Ser.*, 152: 51-66.

- Tsai, A. Y., Chiang, K. P., Chang, J., Gong, G. C., 2005. Seasonal diel variations of picoplankton and nanoplankton in a subtropical western Pacific coastal ecosystem. *Limnol. Oceanogr.*, 50: 1221-1231
- Vaulot, D., Marie, D., 1999. Diel variability of photosynthetic picoplankton in the equatorial Pacific. *J. Geophys. Res.*, 104: 3297-3310
- Vaulot, D., Eikrem, W., Viprey, M., Moreau, H., 2008. The diversity of small eukaryotic phytoplankton ($\leq 3 \mu\text{m}$) in marine ecosystems. *FEMS Microbiol. Rev.*, 32: 795-820
- Wiggert, J., Jones, B., Dickey, T., Brink, K. H., Weller, R. A., Marra, J., Codispoti, L. A., 2000. The Northeast Monsoon's impact on mixing, phytoplankton biomass and nutrient cycling in the Arabian Sea. *Deep Sea Res. II*, 47: 1353-1385
- Wolanski, E., Pickard, G., 1983. Upwelling by internal tides and Kelvin waves at the continental shelf break on the Great Barrier Reef. *Mar. Freshwater Res.*, 34: 65-80
- Wood, H. L., Sundell K., Almroth, B. C., Sköld, H. N., Eriksson, S. P., 2016. Population-dependent effects of ocean acidification. *Proceed. Royal Soc. B*, 283: 1-7
- Worden, A. Z., Nolan, J. K., Palenik, B., 2004. Assessing the dynamics and ecology of marine picophytoplankton: the importance of the eukaryotic component. *Limnol. Oceanogr.*, 49: 168–179.
- Zubkov, M. V., Sleigh, M. A., Tarran, G. A., Burkill, P. H., Leakey, R. J., 1998. Picoplanktonic community structure on an Atlantic transect from 50°N to 50°S. *Deep Sea Res. I*, 45: 1339-1355
- Zwirgmaier, K., Heywood, J. L., Chamberlain, K., Woodward, E. M. S., Zubkov, M. V., Scanlan, D. J., 2007. Basin-scale distribution patterns of picocyanobacterial lineages in the Atlantic Ocean. *Env. Microb.*, 9: 1278-1290

Table 1

Conversion factors used to estimate carbon biomass of PP groups (fg C cell⁻¹) and total phytoplankton ($\mu\text{g C } \mu\text{g}^{-1} \text{ chl } a$) in the mixed layer (ML) and below mixed layer during phase I and phase II.

	Phase I		Phase-II	
	ML	Below ML	ML	Below ML
<i>SYN</i>	106.2	185.1	101.0	152.0
<i>PRO</i>	34.2	84.5	32.0	72.0
PEUK	601.0	647.0	522.0	528.0
C:Chl <i>a</i>	140.0	52.0	83.0	52.0

Table 2

PERMANOVA analysis of environmental variables, PP groups, total phytoplankton carbon biomass, PP carbon biomass, and PP carbon contribution to the total phytoplankton carbon biomass between phase I and phase II samplings in surface waters (0 m), mixed layer (ML) and below mixed layer. Bold text denotes significant variation between the two phases.

Source	Surface waters (0 m)					ML					Below ML				
	df	SS	MS	Pseudo-F	<i>P</i>	df	SS	MS	Pseudo-F	<i>P</i>	df	SS	MS	Pseudo-F	<i>P</i>
Temperature	1	112.6	112.6	3.09	0.00	1	93.6	93.6	11.5	0.01	1	294.1	294.1	2.7	0.09
Salinity	1	91.3	91.3	1.17	0.38	1	14.3	14.3	0.8	0.36	1	0.3	0.3	1.5	0.23
DO	1	337.1	337.1	1.64	0.00	1	78.4	78.4	1.4	0.36	1	11965.0	11965.0	5.3	0.01
NO ₃ ⁻	1	3734.4	3734.4	2.13	0.09	1	13175.0	13175.0	8.8	0.01	1	5385.5	5385.5	5.7	0.01
NO ₂ ⁻	1	1132.9	1132.9	1.05	0.32	1	8364.6	8364.6	7.5	0.01	1	12118.0	12118.0	10.6	0.01
PO ₄ ³⁻	1	799.8	799.8	9.91	0.00	1	4564.1	4564.1	40.0	0.01	1	7061.2	7061.2	19.0	0.01
NH ₄ ⁺	1	729.2	729.2	1.09	0.30	1	4110.1	4110.1	6.8	0.01	1	11460.0	11460.0	15.9	0.01
SiO ₄ ⁴⁻	1	3313.8	3313.8	4.84	0.00	1	2867.8	2867.8	4.1	0.04	1	775.3	775.3	0.8	0.45
Chl <i>a</i>	1	1224.0	1224.0	6.4	0.01	1	3499.6	3499.6	6.2	0.01	1	8887.5	8887.5	7.6	0.01
<i>SYN</i>	1	59.3	59.3	3.08	0.09	1	5026.9	5026.9	5.4	0.01	1	29312.0	29312.0	12.3	0.01
<i>PEUK</i>	1	113.7	113.7	13.01	0.00	1	3886.3	3886.3	6.0	0.01	1	16992.0	16992.0	6.2	0.01
<i>PRO</i>	1	170.2	170.2	8.24	0.01	1	23308.0	23308.0	27.4	0.01	1	2315.9	2315.9	1.2	0.28
Phytoplankton carbon	1	1549.5	1549.5	78.9	0.00	1	5029.7	5029.7	25.4	0.01	1	4256.2	4256.2	15.8	0.01
PP carbon	1	2490.3	2490.3	28.2	0.00	1	7797.3	7797.3	7.8	0.01	1	22374.0	22374.0	16.3	0.01
PP contribution (%)	1	55.5	55.5	1.6	0.23	1	115.1	115.1	0.45	0.64	1	4167.7	4167.7	12.1	0.01

Figure Legends

Fig. 1 Location of sampling station in the eastern Arabian Sea.

Fig. 2 Dot plot of flow cytometric analysis showing PP groups from the eastern Arabian Sea.

Fig. 3 Vertical profiles of temporal variation in (a) temperature, (b) salinity, (c) dissolved oxygen, (d) nitrate, (e) nitrite, (f) orthophosphate, (g) silicate, and (h) ammonium over the continental slope of the eastern Arabian Sea. Black line indicates mixed layer depth.

Fig. 4 Vertical profiles of temporal variation in cell abundance of (a) *SYN*, (b) *PRO*, (c) *PEUK*, and (d) total PP over the continental slope of the eastern Arabian Sea. Black line indicates mixed layer depth.

Fig. 5 Vertical profiles of temporal variation in (a) chlorophyll *a* (b) PP carbon, and (c) PP carbon contribution (%) to the total phytoplankton carbon biomass over the continental slope of the eastern Arabian Sea. Black line indicates mixed layer depth.

Fig. 6 Vertical profiles of temporal variation in (a) *SYN*, (b) *PRO* and (c) *PEUK* carbon contribution to the total PP carbon biomass over the continental slope of the eastern Arabian Sea. Black line indicates mixed layer depth.

Fig. 7 Path diagrams showing the relationships between the environmental variables and PP groups, total phytoplankton carbon biomass, PP carbon biomass, and chl *a* within the mixed layer of phase I (a) phase II (b), below mixed layer at 50 m (c), 75 m (d), 100 m (e), and on day 5 within mixed layer (f) and below mixed layer (g). Bold values are the coefficient of determination of the linear regression (R^2) and colored values are the regression coefficients for the specific standardized independent variables.

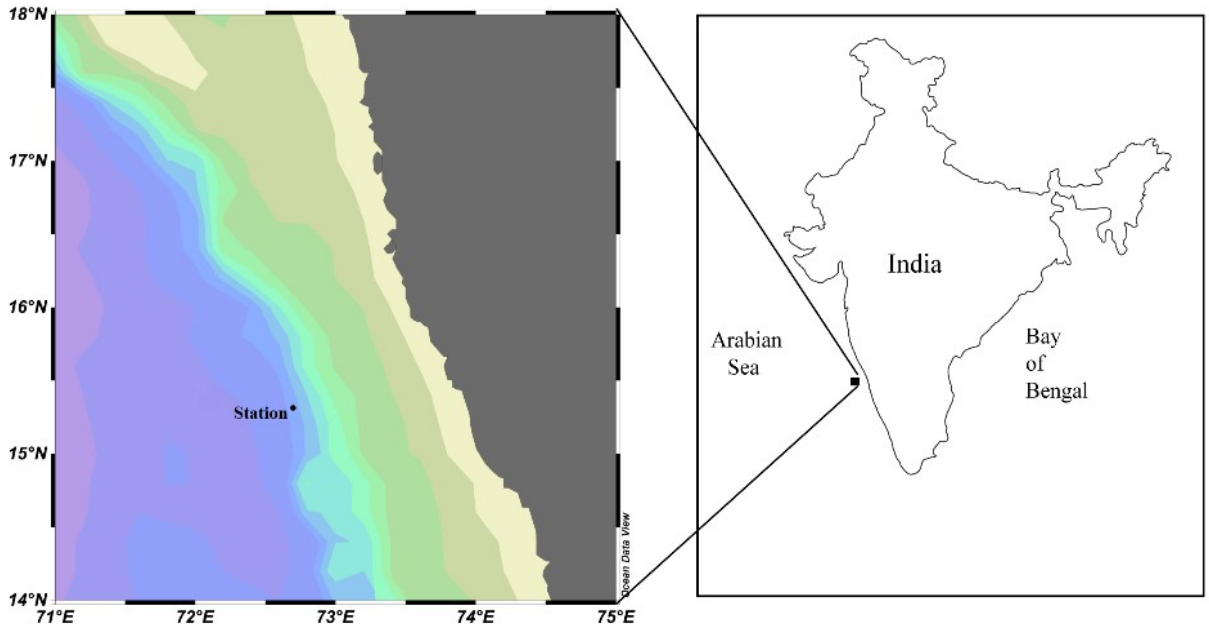


Fig. 1

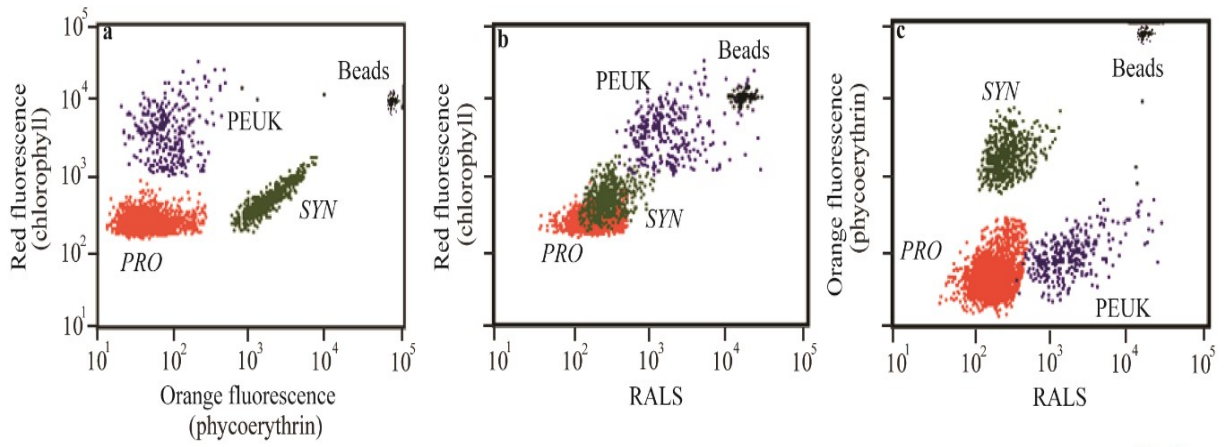


Fig. 2

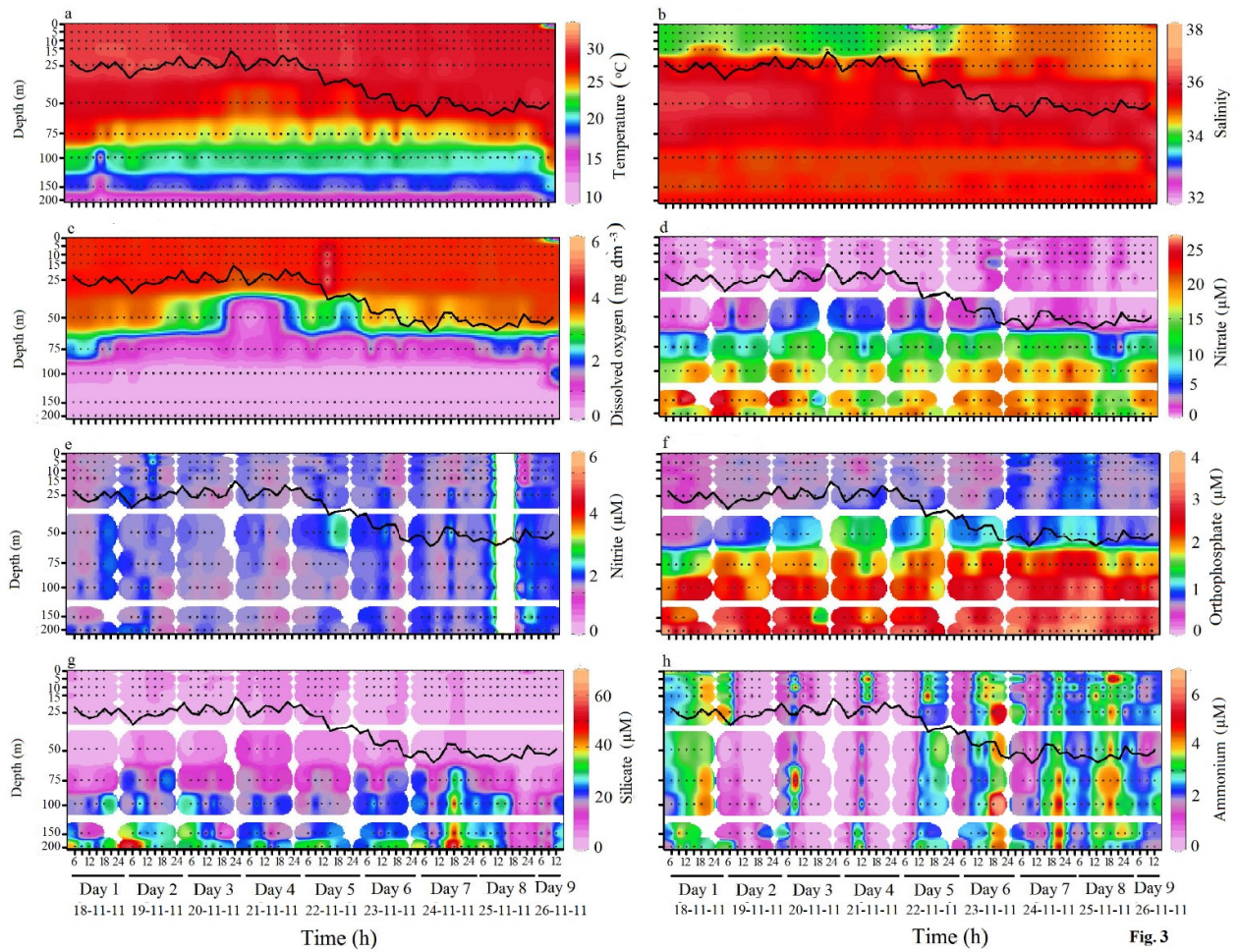


Fig. 3

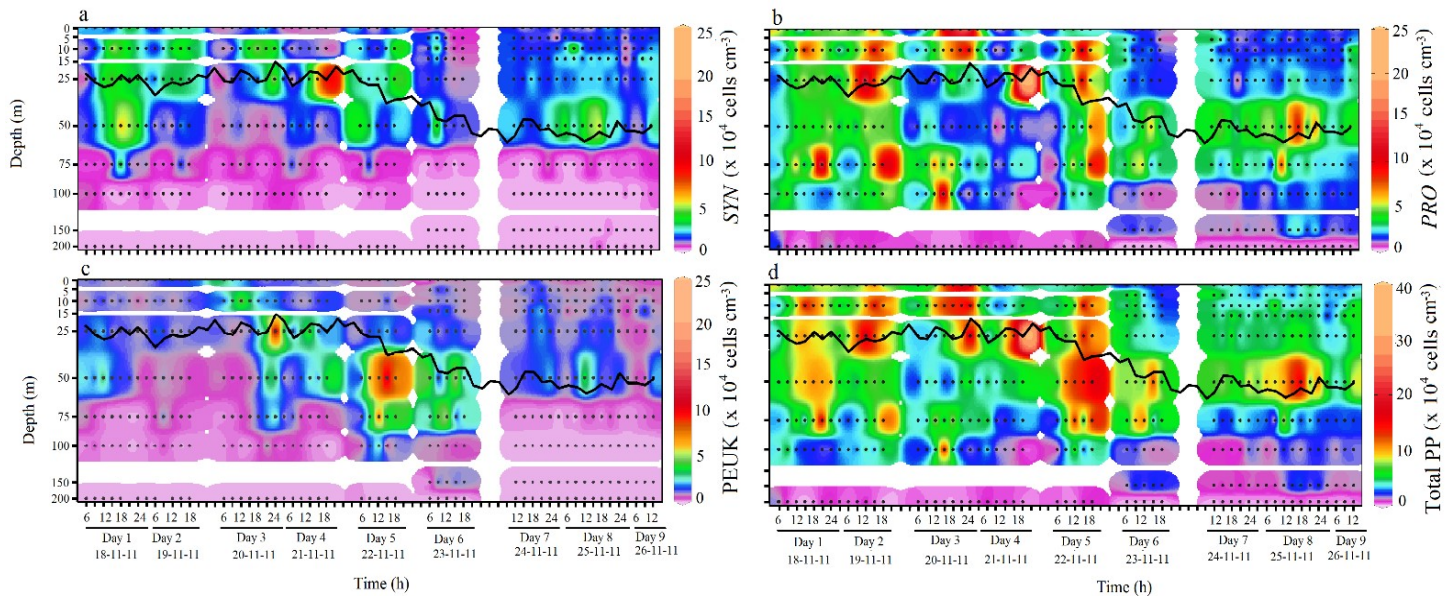


Fig. 4

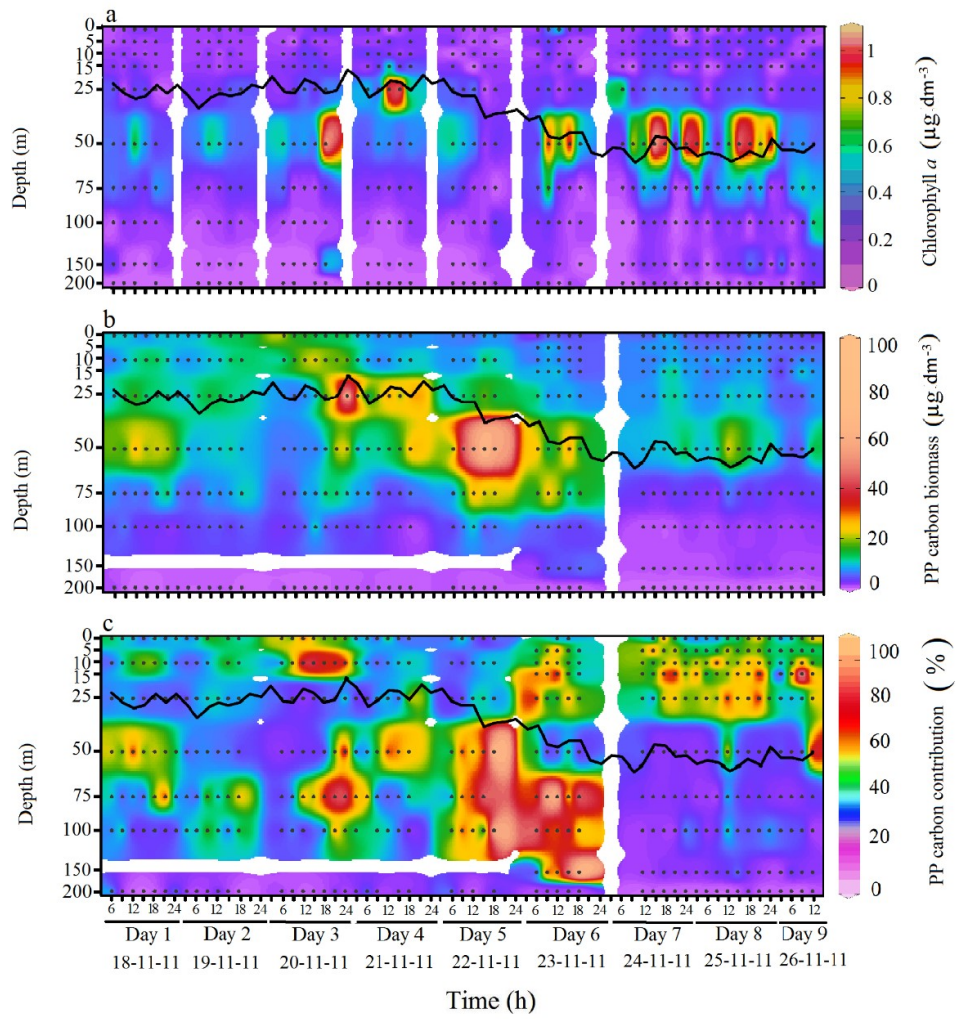


Fig. 5

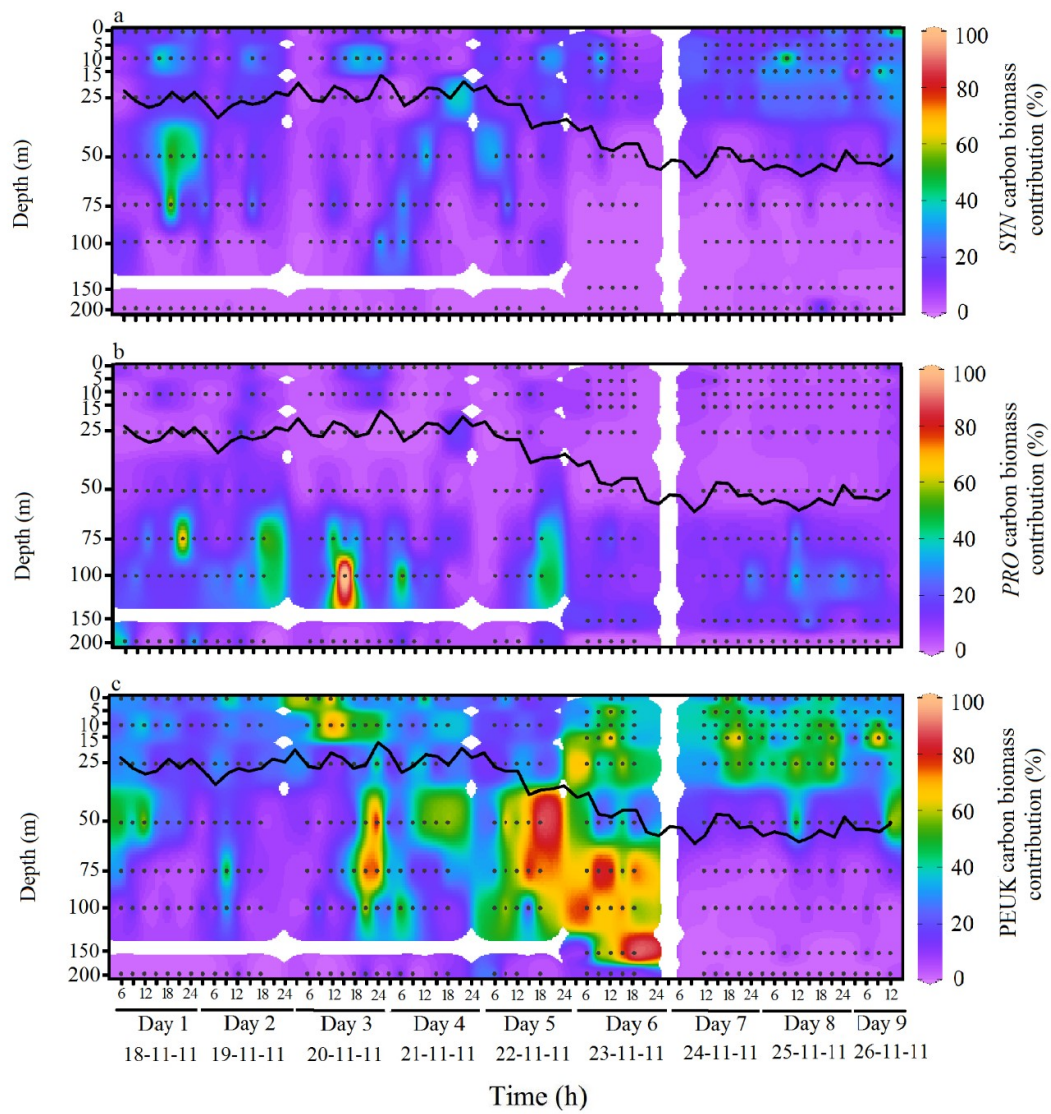


Fig. 6

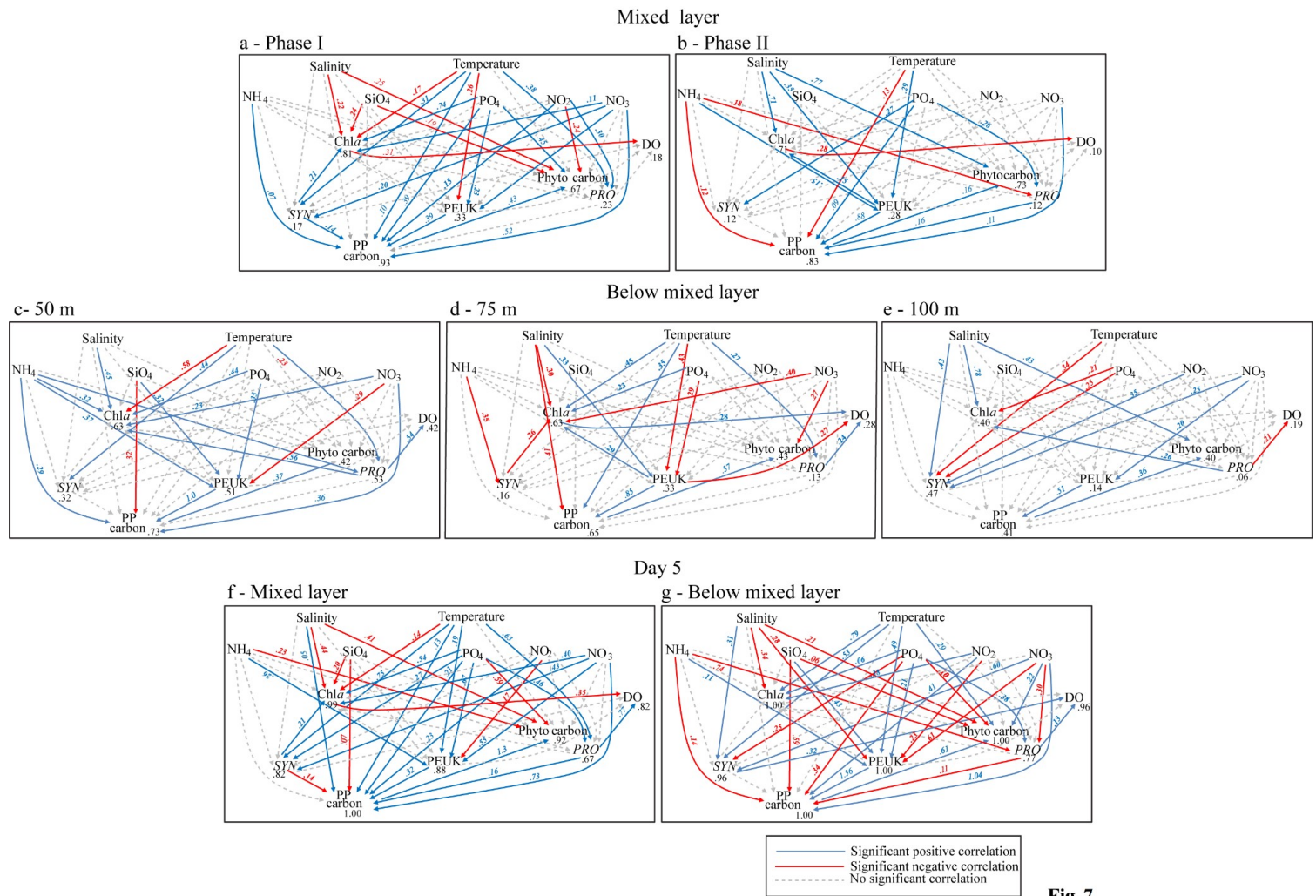


Fig. 7